Performance improvement of Standalone PV system by Full-Bridge LLC Resonant Converter

Dheeban S S[1], Muthu Selvan N B[2], Senthil Kumar C[3], Swapna P[4].
[1,3]Department of Electrical and Electronics Engineering,AAA College of Engineering and Technology, Sivakasi, India.
[2]Department of Electrical and Electronics Engineering, Sri Sivasubramaniya Nadar College of Engineering, Chennai, India.
[4]Department of Electrical and Electronics Engineering, Sri Krishna College of Technology, Coimbatore, India.
Email:[1]dheebanss@ieee.org.

ABSTRACT

The depletion in fossil fuels has turned to increase the rapid exploitation of energy from the Renewable Energy resource. The Renewable Energy resources are intermittent and the reliability can be increased by proper conditioning with power electronic devices. The power electronic devices make use of controllers to change the nature of electrical quantity either AC to DC or vice versa. The DC-DC converters conditions the output energy from sun or wind. Resonant converter works on Zero-Voltage-Switching (ZVS) and Zero-Current-Switching (ZCS). The Full-Bridge LLC resonant converter is a three-element resonant converter that has two inductors coupled together by a capacitor and operates at a high frequency with synchronous self-driven rectifiers. The proposed LLC converter topology minimizes the diode rating enabling the converter to be used for high voltage application. LLC converter ensures switching loss minimization compared to the PWM converters. Photovoltaic panels that harness solar energy make use of MPPT controller and maximum power is extracted. The DC electrical energy fed from the PV panels is conditioned by the Full-Bridge LLC resonant converter that can operate in boost and buck modes. The effectiveness of the converter is calculated through simulation with MATLAB and validation through Hardware-In-Loop.

Keywords
Photo-Voltaic, Resonant converters, MPPT, ZVS, ZCS, Perturb and Observe

Article Received: 10 August 2020, Revised: 25 October 2020, Accepted: 18 November 2020

Introduction

Renewable energy development has led to many DC-DC converter configurations, that can be more efficient in both stand-alone operations and grid-connected operations. The DC-DC converters are used to perform buck, boost operations, load impedance matching, and improve efficiency. The AC load can be connected after conditioning the DC quantity by the DC-DC converter via an inverter [1]. Renewable energy can either be stored in the batteries for future use or the excess of energy can be fed to the grid. In standalone operation the sizing of the batteries is the primary aspect and, in the grid, connected operation synchronizing with the utility grid must of primary concern [2]-[4]. One of the common techniques used to harness maximum energy from the photovoltaic panels is by controlling DC-DC converter switches with the MPPT Controller [5]-[7]. An algorithm is embedded in MPPT controller that tracks the maximum power when there is varying irradiation.
PWM signals are used for generating the control signals for the converter. The converters that are based on PWM signals contribute to switching losses at operation in high voltage. The handling of high voltage with less switching losses in the high frequency domain is possible by the resonant converters. Resonant works on the principle of resonance by coupling two inductors with a capacitor. The resonant converters are easy for magnetic integration, higher efficiency, and soft switching capabilities [8]. The resonant converter can operate at high switching frequencies. The design of the proposed converter, integration with PV, and MPPT controller under load and no-load conditions have been discussed. The Full-Bridge-LLC resonant converter has been compared with boost converter through MATLAB-Simulink and validated through the Hardware-In-Loop process.

Methodology

DC-DC converter has different topologies. Resonant converters are reliable and highly efficient. The Zero Voltage Switching in the resonant converter is responsible for minimization of the switching losses which leads to an increase in operating frequency. The resonant converter is responsible for minimization in switching losses, high power density, and higher operating. The resonant converter is of two types based upon the configuration, Parallel, and Series. In Parallel, the regulation of output voltage is simple as the load is in parallel with the main resonant capacitor. The drawback of Parallel Resonant Converter is that there is an increase in loss of energy as the high circulating current increases. A hybrid combination of Series-Parallel Resonant Converter came into existence which removed the drawbacks of both Series and Parallel.
The proposed LLC resonant converter is made up of a combination of an inductor, capacitor, and inductor [8]-[12]. The proposed LLC resonant converter makes use of the leakage inductance of transformer rather than a resonant inductor. A tank circuit is formed along with a capacitor and the core loss in the transformer is reduced by a reduction in flux ripple. The magnetic component is reduced that minimized the flux ripple. The LLC resonant converter can be classified based on the transformer topology as Center tapped LLC and Full Bridge LLC. Full Bridge LLC reduces the oscillations in voltage at the secondary rectifier due to the secondary leakage inductance [13],[14]. The LLC-

resonant converter modeling is based on [15]. The figure 1 depicts, the LLC Resonant converter with a full-bridge secondary rectifier configuration.

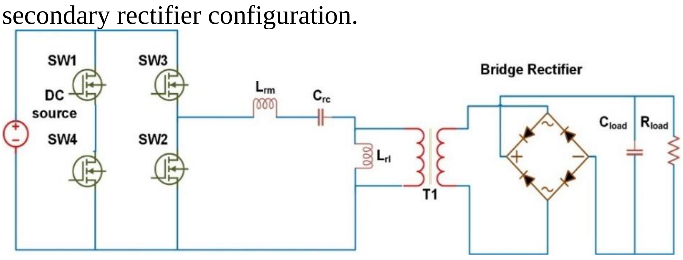

Fig. 1. Full-bridge-LLC Resonant converter with a secondary rectifier

The proposed converter is powered by a DC input, the input bridge configuration is based on the power rating and application [16],[17]. The capacitor C_{rc} coupled together with two inductors, leakage inductor L_{rl}, and magnetizing inductor L_{rm} contributes to the tank circuitry. The resonant tank circuit is responsible for filtering the higher-order harmonics. The tank circuit is made to flow with the fundamental component. The rectified wave is given to the load as output. Two resonant frequencies f_{res1}, f_{res2} corresponding to (L_{rm}+L_{rl}) and C_{rc}, and L_{rl} and C_{rc} respectively. The resonant frequencies are given in equation 1.

$$f_{res1} = \frac{1}{2\pi\sqrt{(L_{rm}+L_{rl})C_{rc}}}$$

$$f_{res2} = \frac{1}{2\pi\sqrt{L_{rl}C_{rc}}}$$

(1)

LLC is a DC-DC converter that can perform both buck and boost operations. Based on the gain the converter function as Series. When the converter operation is above the resonant frequency then the converter gain is below unity. The converter is operated at f_{res2} resonant frequency to achieve higher efficiency and reduction in circulating energy.

Design Methodology

Full-Bridge-LLC resonant converter design is built up on the first-harmonic approximation methodology. The resonant converter is designed to bypass only the fundamental component and the harmonics that are of higher-order will be filtered out. The frequency-dependent parameters like quality factor Qf, normalized frequency f_{nom}, and inductance ratio L_{nr} are used for gain calculation are given in equation 2.

$$f_{nom} = \frac{f_{switch}}{f_{res2}}$$

$$Q_f = \frac{\sqrt{\frac{L_{rl}}{C_{rc}}}}{R_{ac}}$$

$$L_{nr} = \frac{L_{rm}}{L_{rl}} \qquad (2)$$

The gain value M_{gain} is given in equation 3.

$$M_{gain} = \left|\frac{L_{nr}f_{nom}^2}{\{f_{nom}^2(L_n+1)-1\}+jf_{nom}Q_fL_{nr}(f_{nom}^2-1)}\right| \qquad (3)$$

The L_{nr} is a constant value while the f_{nom} parameter is the control variable and the load characterize the value of quality factor Q_f. Based on the suitable L_{nr} and Q_f, the value of minimum gain and maximum gain is given in equation 4.

$$M_{gain\_max} = \frac{V_{input\_nom}}{V_{input\_min}}$$

$$M_{gain\_min} = \frac{V_{input\_nom}}{V_{input\_max}} \qquad (4)$$

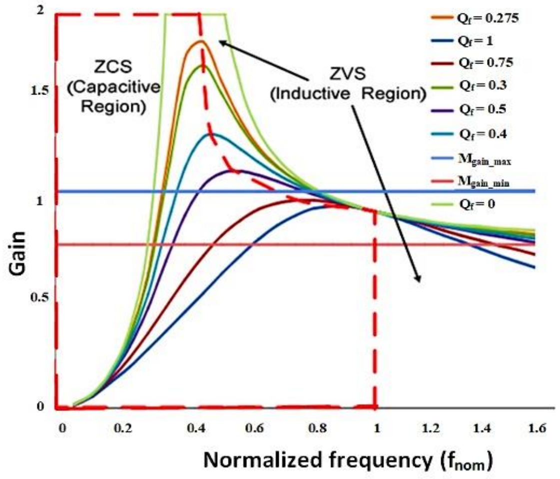

Fig. 2. Resonant converter Gain Characteristics

Gain characteristics is shown in figure 2. Q_f, and L_{rn} parameter selection contribute to the reactive components. The gain characteristics imply that the ZCS operation performed at the capacitive region and the ZVS performed in the inductive region. AC equivalent resistance value is given in equation 5.

$$R_{ac} = \frac{8R_l n^2}{\pi^2} \qquad (5)$$

Higher magnetizing current is obtained by reducing the value of L_{rm} and L_{rm} is 20% below the primary current. C_{rc}, L_{rl}, and L_{rm} are selected from equations 6,7 and 8.

$$C_{rc} = \frac{1}{2\pi f_{res2}Q_fR_{ac}} \qquad (6)$$

$$L_{rl} = \frac{1}{(2\pi f_{res2})^2C_{rc}} \qquad (7)$$

$$L_{rm} = L_{nr}L_{rl} \qquad (8)$$

The transformer plays an important role in the resonant. The minimum number of primary windings in a transformer is given by equation 9.

$$N_{p\_min} = \frac{n(V_{out}+2V_f)}{2f_{min\_switch}\Delta B.A} \qquad (9)$$

A- Area of the core of the transformer, B- Magnetic flux density, f_{min_switch}- the minimum switching frequency.

The number of primary windings must be greater than the number of minimum primary windings. The ZVS switching involves, tuning of MOSFET switches at the time of drain to source voltage V_{DS} remains zero. The inductive energy required is delivered by the magnetizing inductor L_{rm}. The value of peak magnetizing current for magnetizing operation is given in equation 10.

$$I_{peak} = \frac{nV_{out}T}{4L_{rm}} \qquad (10)$$

ZVS operation can be achieved when the value of L_{rm} is small and the L_{rm} selection is given by equation 11.

$$L_{rm} = \frac{Tt_d}{16C_{jnc}} \qquad (11)$$

C_{jnc} – junction capacitance, T_d – Dead Time

PV Integration

The LLC resonant converter boosts the voltage from the array of PV panels. The entrapped solar energy at the PV panel is converted to electrical energy and fed to the LLC resonant converter. Single diode PV cell is the simplest and commonly used modeling method of PV panels [2]. The single diode PV cell equivalent circuit is given in figure 3.

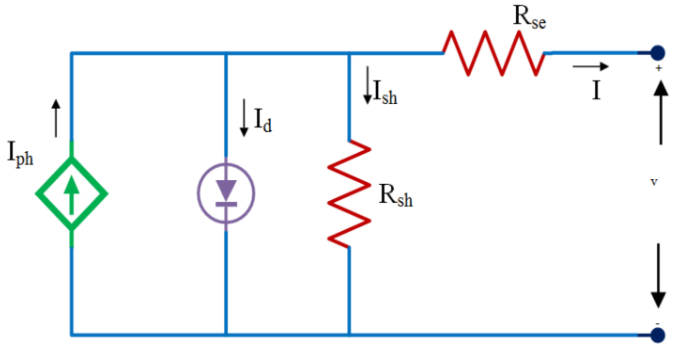

Fig. 3. Single Diode PV Cell

The PV panels can be characterized by the I-V graph and P-V graph which are given in figure 4.

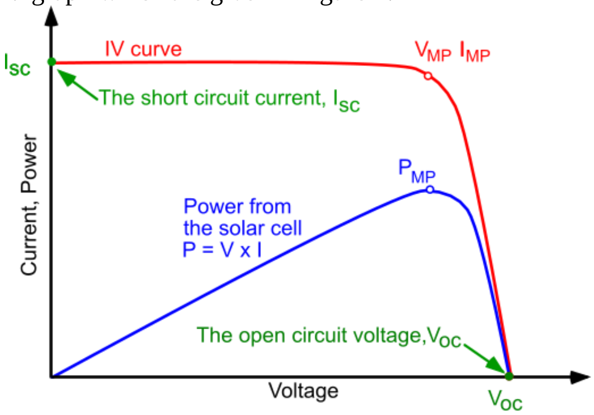

Fig. 4. P-V and I-V characteristics of Photovoltaic panels

The P-V graph and I-V graphs determine the maximum power. The power extracted from the PV panels is intermittent and it is not constant due to varying irradiation levels. The block diagram of the integration of a resonant converter with the PV array is given in figure 5.

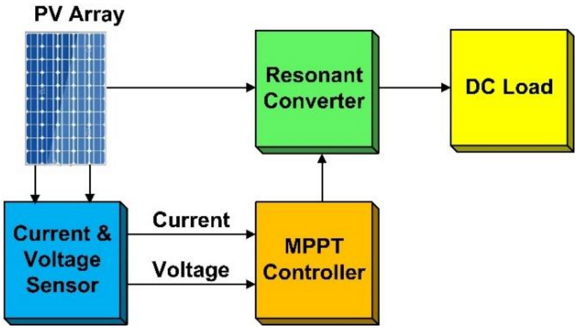

Fig. 5. Resonant converter integration to PV panels

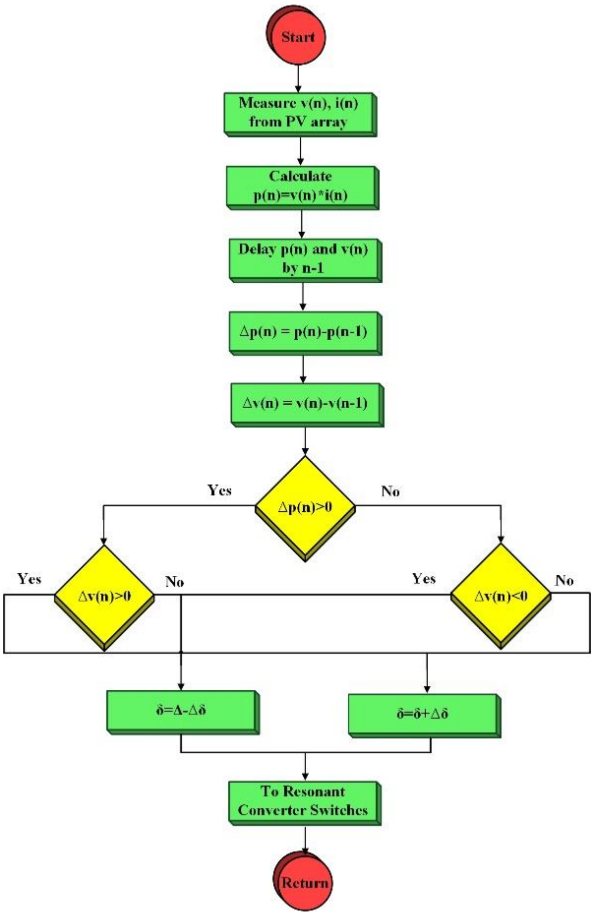

Fig. 6. Perturb & Observe algorithm

The MPPT controller power extraction is based on P& O algorithm. The PV module is given a small perturbation which induces changes in power. The decrease in voltage level tends to decrease the power and the operating point in the P-V graph tends to move towards the left of the P-V curve. Hence, to attain maximum power the MPP must be moved towards the right. Similarly, the increase in voltage level tends to increase the power and the operating point in the P-V graph tends to move towards the right of the P-V curve [2]-[4]. Hence, to attain maximum power the MPP must be moved towards the left. The flow chart of P&O algorithm is given in figure 6.

Results and Discussion

Simulation Results

The P-V panel and the LLC resonant converter are modelled in MATLAB-Simulink and the performance has been compared with the conventional boost converter. The Photovoltaic panel can be characterized by the maximum peak voltage V_{mpeak}, maximum peak current I_{mpeak}, open circuit voltage $V_{open\_circuit}$ and short circuit current $I_{short\_circuit}$. The parameters of the PV panel are specified in Table 1.

Table 1. PV panel and LLC Resonant converter parameters for MATLAB Simulation

Parameters	Values
Resonant Converter	
DC Input voltage V_{input}	40V
Magnetizing Inductor L_{rm}	92.50µH

Leakage Inductor L_{rl}	61.97µH
Resonant Capacitor C_{rc}	0.052µF
Output Capacitor C_{load}	120µH
Load Resistance R_{load}	42Ω
Resonant Frequency f_{res}	10kHz
Switching Frequency f_{sw}	1kHz
PV Panel	
Peak Voltage V_{mpeak}	36V
Peak Current I_{mpeak}	5A
Open Circuit Voltage $V_{open\_circuit}$	44.8V
Short Circuit Voltage $I_{short\_circuit}$	5.35A
Maximum Power P_{max}	180W

The P-V and I-V graphs obtained for various irradiation at a constant temperature of 25ºC for the PV module is in figure 7.

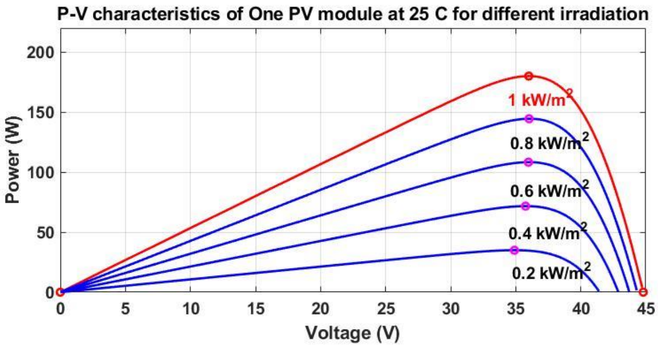

(a)

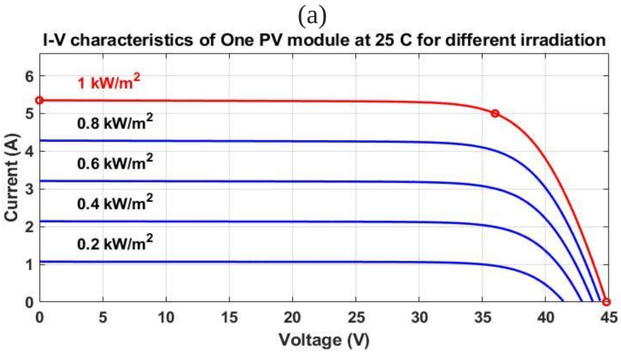

(b)

Fig. 7. (a) P-V, (b) I-V of one PV module at 25ºC for various irradiation

The P-V and I-V graphs obtained for different temperatures at an irradiation of 1000 W/m^2 is in figure 8.

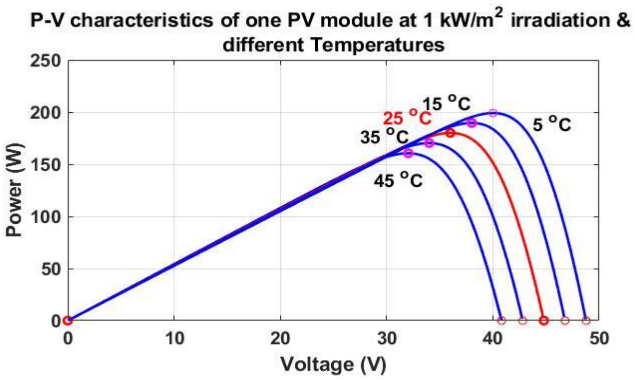

(a)

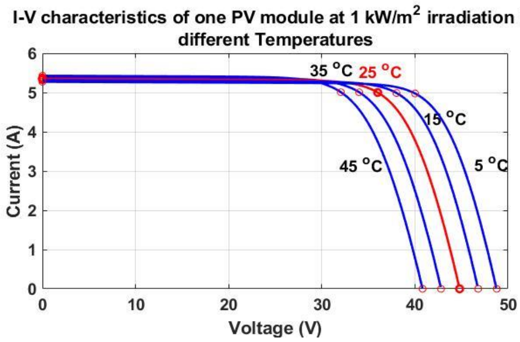

(b)

Fig. 8. (a) P-V, (b) I-V of one PV module at 1 kW/m^2 irradiation for various temperatures

The PV panel is coupled to a DC-DC Full Bridge Resonant converter. PV panel output is 40V and PV panel voltage is conditioned and boosted up to a voltage level of 80V by the resonant converter. The output voltage is given in figure 9.

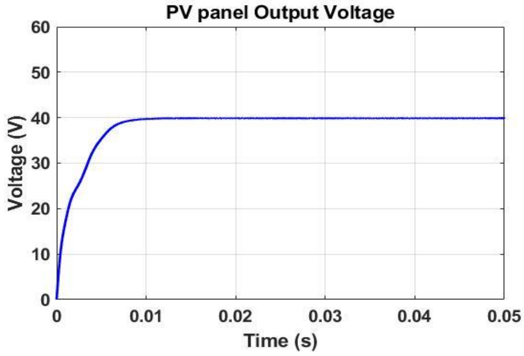

Fig. 9. PV panel output

The voltage and current from the resonant converters are given in figures 10 and 11.

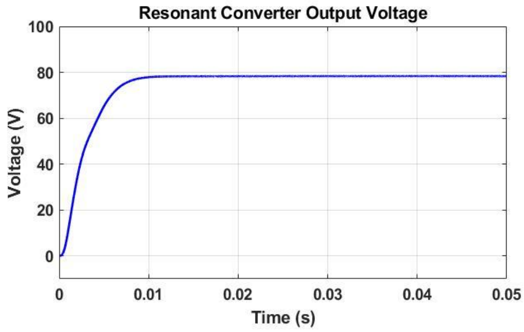

Fig. 10. Resonant Converter Output voltage

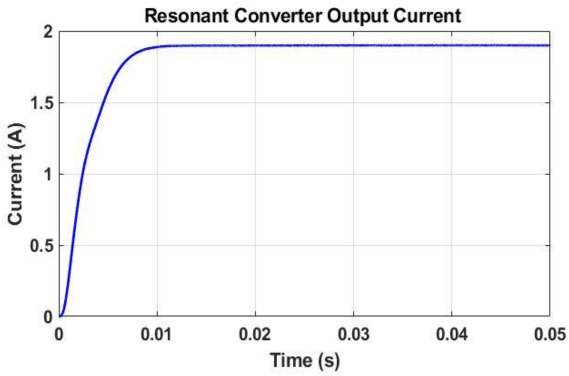

Fig. 11. Resonant converter Output current

The power output delivered by the resonant converter is given in figure 12. Efficiency is compared with the most commonly used solar panel integrated to a boost converter configuration. The resonant converter performs more efficiently than the boost converter which is evident from figure 13.

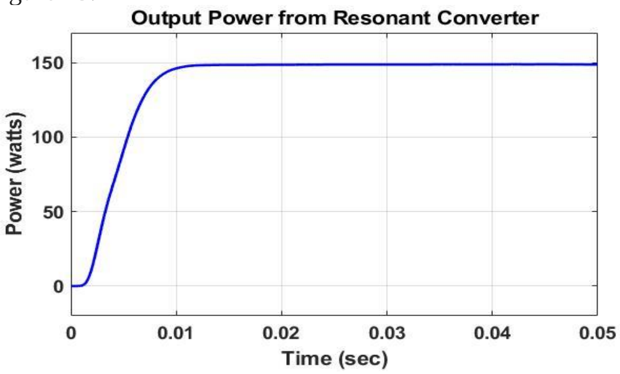

Fig. 12. Output power from the Resonant converter

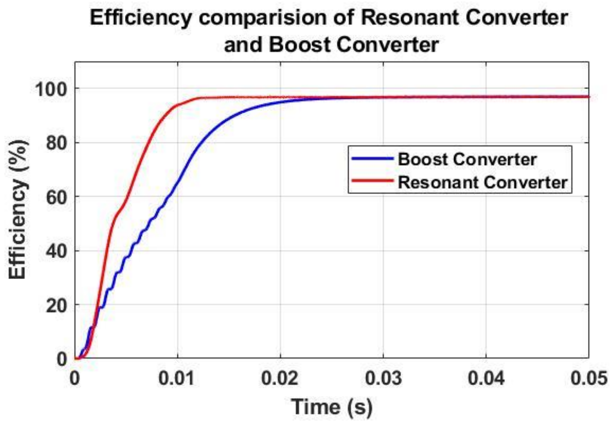

Fig. 13. Efficiency comparison between Resonant Converter and Boost Converter

In the resonant converter, the switching process is ZVS and ZCS, compared with normal switching in boost converters, the switching losses are minimized in a resonant converter. The efficiency got from the resonant converter is around 96.7%.

Experimental Validation

The LLC resonant converter has been simulated in boost mode for comparing with the traditional boost converter and the efficiency is superior to the boost converter due to the reduction in switching losses and less voltage stress. The PV powered LLC resonant converter has been experimented and validated through Hardware-In-Loop device like Typhoon HIL 603. The LLC resonant converter is made to run over the HIL device while the PV is emulated via the core of the CPU. The specification of the PV panel and the resonant converter are shown in table 2.

Table 2 PV panel and LLC Resonant converter parameters for HIL validation

Parameters	Values
Resonant Converter	
DC Input voltage V_{input}	400V
Magnetizing Inductor L_{rm}	0.285µH
Leakage Inductor L_{rl}	0.856µH
Resonant Capacitor C_{rc}	0.888nF
Output Capacitor C_{load}	560µH
Load Resistance R_{load}	80Ω
Resonant Frequency f_{res}	10kHz
Switching Frequency f_{sw}	1kHz
PV Panel	
Peak Voltage V_{mpeak}	36V
Peak Current I_{mpeak}	5A
Open Circuit Voltage $V_{open\_circuit}$	44.8V
Short Circuit Voltage $I_{short\_circuit}$	5.35A
Maximum Power P_{max}	180W

The proposed converter is validated for the buck mode of operation where the 400V input voltage from the PV panels is stepped down to a voltage of 12V. PV panel is designed to output a voltage of 400V and power of 2kW. The PV module is of 72 cells and 9 PV panels are connected in series to generate a voltage of 400V and a single PV panel is connected in parallel to generate a maximum current of 5A. The LLC resonant converter characteristics are observed for two cases as follows.

1. Case-1: No Load Condition
2. Case-2: Load Condition

Case 1: No Load Condition

In case 1, the LLC resonant converter integrated with PV, and there is no load connected to the system. The input DC voltage from the PV panels is converted to AC quantity via the inverter circuit and the switching employed is Zero Voltage Switching where the voltage in the switching device is forced to zero voltage due to the resonance. The input voltage is kept constant by having constant irradiation of 1000W/m^2. There is no load connected to the system hence the current in load is zero. The voltage and current from inverter, current through the switches I_{sw1}, I_{sw2}, I_{sw3} and I_{sw4}, and voltage and current through load are shown in figure 14.

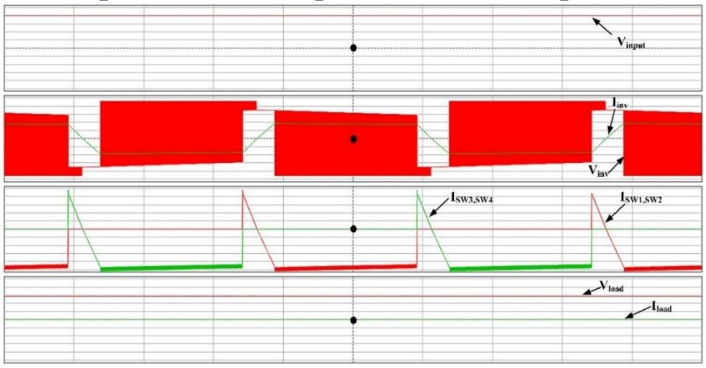

Fig. 14. Input Voltage V_{input}: 100V/div, Inverter Voltage V_{inv}:50V/div, Inverter current: 500mA/div, Current in IGBTs: 200mA/div, Load Voltage V_{load}: 5V/div, Load Current I_{Load}: 0A/div and Time base: 200µs in no-load condition

During the no-load condition, output voltage from inverter is distorted and the resonant current is equal to the circulating current. The excess voltage appears across L_{rl} inductor as in no-load which causes the switching frequency to be doubled than the resonant frequency. The resonant current I_{res} flows in the first half cycle and the magnetizing current I_m in figure 15.

Fig. 15. Resonant Current I_{res}: 500mA/div, Magnetizing current I_m: 500mA/div, Inverter PWM switching Pulse varying from 0 to 1V ($V_{pulse\_SW1,SW2}$ and $V_{pulse\_SW3,SW4}$) and Timebase: 200µs in no-load condition

During the first half cycle, the magnetizing current remains constant and in the next half-cycle, it reduces linearly to reach the negative maximum. As there is no load, there is no flow of load current and the resonating current is distorted and it is non-sinusoidal in nature.

Case 2: Load condition

In case 2, the load is connected. A constant DC input of 400V is supplied from PV panels. Input DC voltage at constant irradiation of 1000W/m^2, the current through the inverter switches, inverter voltage, and current and voltage and current at load are shown in figure 16.

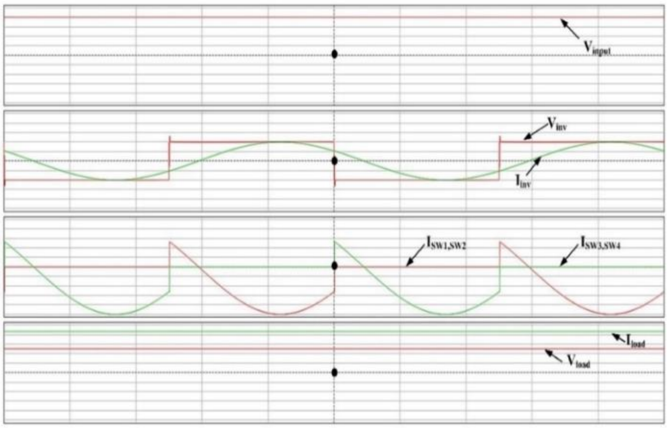

Fig. 16. Input Voltage V_{input}: 100V/div, Inverter Voltage V_{inv}:100V/div, Inverter current: 5A/div, Current in IGBTs: 2A/div, Load Voltage V_{load}: 5V/div, Load Current I_{Load}: 20A/div and Timebase: 200µs in load condition

During load condition, the voltage and current from the inverter are 200V and 7A respectively. The current and voltage through the load are 12V and 83A respectively. The load current flows as the full load is connected and there resonating current flow I_{res} and the magnetizing current I_m are shown in figure 17.

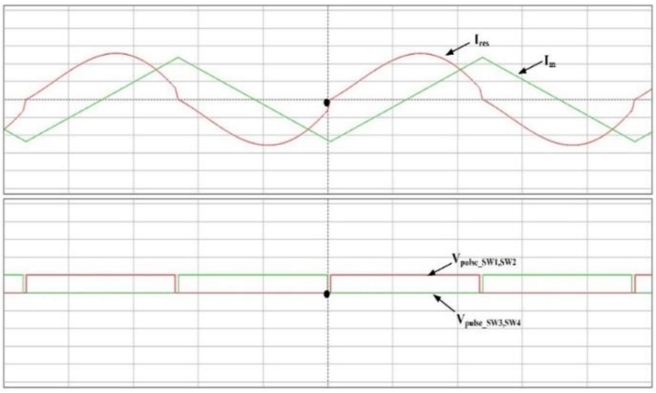

Fig. 17. Resonant Current I_{res}: 50A/div, Magnetizing current I_m: 2A/div, Inverter PWM switching Pulse varying from 0 to 1V ($V_{pulse\_SW1,SW2}$ and $V_{pulse\_SW3,SW4}$) and Timebase: 200µs in load condition

During full load condition, the input voltage 400V is stepped down to supply the load with 12V and from figure 17 it can be inferred that the resonant current is sinusoidal while the current through the magnetizing inductor increases linearly in the first-half-cycle and decreases in the second-half-cycle. Due to the flow of load current, there are no distortions in resonant current I_{res}. The ZVS operation can be achieved in any load condition as the current through magnetizing inductor decides the turn off period. The irradiation from the PV is reduced from 1000W/m^2 to 800W/m^2, which tends to reduce the input voltage. The various waveforms with respect to the resonant converter in the reduction of irradiation are shown in figure 18.

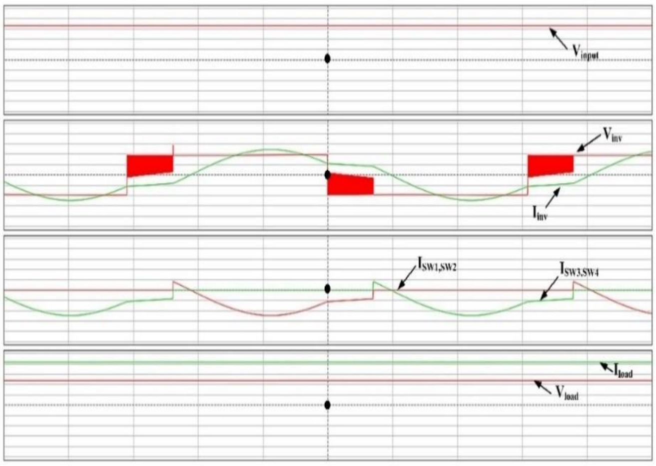

Fig. 18. Input Voltage V_{input}: 100V/div, Inverter Voltage V_{inv}:100V/div, Inverter current: 5A/div, Current in IGBTs: 5A/div, Load Voltage V_{load}: 5V/div, Load Current I_{Load}: 20A/div and Time base: 200µs in load condition during varying irradiation

The irradiation is varied and the PV panel inputs a voltage of 330V for irradiation of 800W/m^2, the switching pulse to the inverter is given from the MPPT controller which is embedded with Perturb and Observe algorithm. The inverter output voltage is 194V and the inverter output current is 10A. The output load voltage is maintained at 12V and the current is at 83A. The resonant current I_{res} and magnetizing current I_m due to change in irradiation are shown in figure 19.

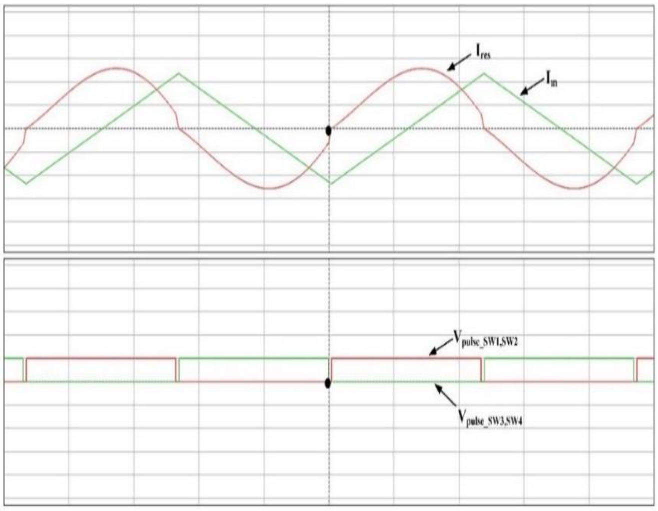

Fig. 19. Resonant Current I_{res}: 50A/div, Magnetizing current I_m: 2A/div, Inverter PWM switching Pulse varying from 0 to 1V ($V_{pulse\_SW1,SW2}$ and $V_{pulse\_SW3,SW4}$) and Timebase: 200μs in load condition during varying irradiation

As the irradiation is varied the input voltage gets reduced and the resonant current I_{res} tends to be less sinusoidal. The magnetizing current I_m remains as increases and decreases linearly. As the input voltage decreases, there is an increase in the circulating current which tends to increase the conduction losses. The resonant current is more sinusoidal in high input voltage (figure 17) than reduced input voltage (figure 19). As the switches operate due to the ZVS operation, the switching frequency is lesser than the resonant frequency. The lower value of switching frequency minimizes the losses at the rectifier diode by reducing the reverse recovery loss of the diodes on the rectifier side. Hence the Full Bridge LLC resonant converter can operate at very high voltage with reduced losses and eliminates the use of secondary inductor.

Conclusion

Renewable energy resources are the major replacement for conventional energy resources. Solar energy integration is exponentially growing in developed countries. PV panel output is intermittent, hence the power has to be conditioned before feeding to the load. The DC-DC converters are used for conditioning purpose and the most commonly used converter is the boost converter. The resonant converters can replace the boost converters as the switching losses are minimum in resonant converters and this increases the efficiency of the entire system.

- The proposed topology of the converter has been employed to achieve higher efficiency and limit the circulating current at higher frequencies.
- The PV supply conditioned during two cases, on load condition and no-load condition.
- The variation in irradiations has been enumerated and fed to the MPPT controller.

The efficiency of resonant converters can be improved further by the use of Silicone Carbide switches. The PV integrated full bridge resonant converter can be used for electric vehicle charging in charging stations.

References

[1] W. M. Grady, M. J. Samotyj, and A. A. Noyola, (1990). Survey of active power line conditioning methodologies. IEEE Trans. Power Del., vol.5, no. 3, July, pp. 1536–1542.

[2] Dheeban S S, Muthu Selvan N B, Senthil Kumar C, (2019). Design of Standalone Pv System. International Journal Of Scientific & Technology Research, Volume 8, Issue 11, November, pp. 684-688.

[3] S.S Dheeban, and V. Kamaraj, (2016). Grid Integration of 10kW Solar Panel. 3rd International Conference on Electrical Energy Systems, pp. 257-266.

[4] S. S. Dheeban, N. B. Muthu Selvan and L. Krishnaveni, (2020). Performance improvement of Photo-Voltaic panels by Super-Lift Luo converter in standalone application. Materials Today: Proceedings. https://doi.org/10.1016/j.matpr.2020.06.352.

[5] S. S. Dheeban and N. B. Muthu Selvan, (2020), PV integrated UPQC for sensitive Load. International Conference on Emerging Trends in Information Technology and Engineering (ic-ETITE), Vellore, India, pp. 1-7. https://doi: 10.1109/ic-ETITE47903.2020.330.

[6] Dheeban S S, N. B. Muthu Selvan and L. Krishnaveni, “Performance improvement of Photo-Voltaic panels by Super-Lift Luo converter in standalone application”, Materials Today: Proceedings, https://doi.org/10.1016/j.matpr.2020.06.352.

[7] Dheeban S S, Muthu Selvan N B and Umashankar Subramaniam, “Power conditioning of standalone Photo-voltaic system with BLDC motor by Negative-Output Luo Converter”, International conference on Power Electronics and Renewable Energy Applications 2020 (IEEE-PEREA2020).

[8] Bhuvaneswari C., & Babu, R. S. R. (2016). A review on LLC Resonant Converter, International Conference on

Computation of Power, Energy Information and Communication (ICCPEIC). doi:10.1109/iccpeic.2016.7557268.

[9] X.F. Shi, C.Y. Chan, (2002). A passivity approach to controller design for quasi-resonant converters. Automatica, vol. 38, pp. 1727, 2002.

[10] S. E. Lyshevski, (2000). Resonant converters: nonlinear analysis and control. IEEE Transactions on Industrial Electronics, vol. 47, no. 4, August, pp. 751-758. doi: 10.1109/41.857955.

[11] Wen-Jian Gu and K. Harada, (1988). A new method to regulate resonant converters. IEEE Transactions on Power Electronics, vol. 3, no. 4, October, pp. 430-439. doi: 10.1109/63.17964.

[12] Lee and G. Moon, (2014). The k-Q Analysis for an LLC Series Resonant Converter. IEEE Transactions on Power Electronics, vol. 29, no. 1, January, pp. 13-16. doi: 10.1109/TPEL.2013.2255106.

[13] Nathan, B. S., & Ramanarayanan, V, (2000). Analysis, simulation and design of series resonant converter for high voltage applications. Proceedings of IEEE International Conference on Industrial Technology (IEEE Cat. No.00TH8482). doi:10.1109/icit.2000.854252.

[14] Yu, S.-Y. (2016). A new compact and high efficiency resonant converter. IEEE Applied Power Electronics Conference and Exposition (APEC). doi:10.1109/apec.2016.7468218..